Chinese Journal of Chemical Engineering 54 (2023) 296–305

Contents lists available at ScienceDirect

Chinese Journal of Chemical Engineering

journal homepage: www.elsevier.com/locate/CJChE

Full Length Article

The superhydrophobic sponge decorated with Ni-Co double layered oxides with thiol modification for continuous oil/water separation

Xiaodong Yang [#], Na Yang [#], Ziqiang Gong, Feifei Peng, Bin Jiang, Yongli Sun, Luhong Zhang [*]

School of Chemical Engineering and Technology, Tianjin University, Tianjin 300072, China

ARTICLE INFO

Article history:
Received 15 November 2021
Received in revised form 13 March 2022
Accepted 15 March 2022
Available online 22 April 2022

Keywords:
Superhydrophobic sponge
Ni-Co double layered oxides
Thiol modification
Oil absorption
Oil/water separation

ABSTRACT

In this paper, the superhydrophobic polyurethane sponge (SS-PU) was facilely fabricated by etching with Jones reagent to bind the nanoparticles of Ni-Co double layered oxides (LDOs) on the surface, and following modification with *n*-dodecyl mercaptan (DDT). This method provides a new strategy to fabricate superhydrophobic PU sponge with a water contact angle of 157° for absorbing oil with low cost and in large scale. It exhibits the strong absorption capacity and highly selective characteristic for various kinds of oils which can be recycled by simple squeezing. Besides, the as-prepared sponge can deal with the floating and underwater oils, indicating its application value in handling oil spills and domestic oily wastewater. The good self-cleaning ability shows the potential to clear the pollutants due to the ultra-low adhesion to water. Especially, the most important point is that the superhydrophobic sponge can continuously and effectively separate the oil/water mixture against the condition of turbulent disturbance by using our designed device system, which exhibit its good superhydrophobicity, strong stability. Furthermore, the SS-PU still maintained stable absorption performance after 150 cycle tests without losing capacity obviously, showing excellent durability in long-term operation and significant potential as an efficient absorbent in large-scale dispose of oily water.

1. Introduction

Serious leakage of crude oil and organic solvents causes frequent water pollution incidents, which severely break ecological balance and threaten human health [1–3]. Thus, the realization of separation and collection from oil sewage is extremely urgent, which has attracted great attention all over the world. Currently, various materials have been studied to address the problems of oil spill and oily water discharge [4]. Different from the traditional 2D materials for simply separating oil/water mixture, including the polymer membrane [5], carbon cloth [6] or metal mesh [7], the 3D porous absorbent materials own excellent adsorption performance, which has aroused considerable interests. The traditional absorbent materials for treating these oil slicks are bentonite [8], zeolite [9], activated carbon [10], plant straw [11] and cotton fibers [12], *etc*. However, there are still many drawbacks which restrict the developments and practical application in oil removal, such as weak adsorption capacity, poor cycle performance, and high fabrication cost. And the most of 3D porous absorbent materials are limited by poor reusability, bad oil absorption capacity, short service life, *etc*. [13].

Layered double hydroxides (LDHs), a large family of two dimensional (2D) anionic clay materials, are composed of brucite-like layers in which a fraction of the divalent (M^{2+}) and trivalent metal cations (M^{3+}) [14]. The versatile types of metal cations, the M^{2+}/M^{3+} molar ratios, and the properties of interlaminar compensating anions lead to various host–guest assemblies and nanostructures. Due to their strengths in easy fabrication, flexible composition, and chemical multifunctionality, LDHs have attracted great attentions in various fields such as catalysis [15], separation [16], adsorbents [17]. Additionally, LDHs can be frequently synthesized by co-precipitation and anion-exchange, and memory effect method [18]. Among these candidates, Ni-Co LDHs based nanostructures have a promising potential for use due to their low cost, and environmentally-friendly nature [19]. In fact, LDHs have been studied as precursors with nano architectures in oil/water separation due to the facile tunability of morphologies and chemical compositions [20]. The calcination treatment enables the removal of

* Corresponding author: Fax: +86 22 27400199.
E-mail address: zhanglvh@tju.edu.cn (L. Zhang).
[#] These authors contribute equally to this work.

https://doi.org/10.1016/j.cjche.2022.03.023

water and hydroxyls from LDH accompanied by the solid phase conversion to layered double oxides (LDOs). [21] LDOs acquired by calcination of LDHs typically has large surface area, enhanced dispersed active ingredient, the advantages of low toxicity and cost, strong stability, *etc*., which has been widely studied in the treatment of organic pollutants. [22] Thus, we envisage to fabricate the superhydrophobic sponge utilizing Ni-Co LDOs derived from LDHs as rough coating with low cost and in large amounts.

Polyurethane (PU) sponge has the advantages of high porosity, low cost and super elasticity, facile fabrication, which has gradually become ideal absorbent materials for oil absorption [23]. For example, our group reported a superhydrophobic PU sponge through a combined method of interfacial polymerization (IP) and molecular self-assembly, which has high oil absorption capacity, good mechanical strength, and reusability in oil/water separation [4]. In fact, the surface of PU sponge is usually hydrophilic attributed to the carboxyl and amino groups. Nevertheless, an effective way to fabricate superhydrophobic surface on the hydrophilic sponge skeleton is building rough structure followed by hydrophobic coating. For example, our group fabricated superhydrophobic PU sponge based on the method of interfacial polymerization and molecular self-assembly, showing robust and durable property for oil/water separation [24]. In addition, Jiang *et al.* [25] prepared PU@Fe_3O_4@PS sponge through ultrasonic dip-coating and self-initiated photografting and photopolymerization, which could be recycled by a magnet conveniently. However, this work offers a new way based on the following study to prepare oil absorbent materials with higher water contact angle (157°). Notably, the active etching of polyurethane surface can be accomplished facilely by H_2SO_4, $H_2Cr_2O_7$ or $SnCl_2$ [26–28], *etc*. It has been proved that the activated PU sponge can both generate specific micro/nanoscale multilevel roughness on the surface, and produce some hydrophilic groups, such as —COOH and —OH [29,30]. In addition, some researches have confirmed that the oxides corresponding to the transition metal elements of the VIII group can strongly interact with the polar group ligand (O, N, S), which improve the binding force of the oxide nanoparticles with the sponge substrate, and are modified easily by chemicals of low surface energy [27,31]. Therefore, the etching could both produce vast oxygen-containing groups and create rough structure, which make PU sponge with large surface area absorb and firmly combine with Ni-Co LDOs by polar groups. By reasonably controlling the etching time, rough structure can be fabricated easily on the surface, which greatly strengthen adsorption of transition metal oxide nanoparticles derived from Ni-Co LDHs.

In this paper, we employ the Jones reagent to etch the original PU sponge surface for building rough surface and supplying polar groups. The loading of Ni-Co double layered oxides (LDOs) nanocrystals on the surface of activated sponge is realized by one step dip-coating. Through the modification with DDT, the superhydrophobic sponge can be fabricated, which could both effectively deal with floating oil, and quickly absorb heavy oil in water. Besides, the superhydrophobic sponge had excellent self-cleaning performance for its ultra-low adhesion to water. By using our designed device system, the as-prepared sponge exhibited continuous absorption and removal of oil contaminants from water with high efficiency even under the harsh disturbance, showing outstanding hydrophobicity, strong robustness. The facile synthetic process ensured the integrity of the SS-PU sponge structure, effectively strengthening the stability of the material. In addition, after 150 cycles of oil absorption tests, it still had high absorption capacity, and maintained complete hierarchical structure. In summary, the functionalized sponge in this study displayed excellent reusability and durability of oil absorption, providing a prominent candidate in long-term operation for large-scale oil–water separation and oil recyclability.

2. Experimental

2.1. Materials

All reagents were of analytical grade and used without further purification. PU sponge (size 10 mm × 10 mm × 30 mm) was purchased from Hangmei company (Hangzhou, China). Acetone, H_2SO_4 (98% (mass)), $Ni(NO_3)_2{\cdot}6H_2O$ and $Co(NO_3)_2{\cdot}6H_2O$ were obtained from Jiangtian Chemical Technology Co., Ltd (Tianjin, China). Chromium oxide (CrO_3, 99.9% (mass)) was purchased from Shanghai Macklin Biochemical Co., Ltd (Shanghai, China). Hexamethylenetetramine (99% (mass)) was supplied by Shanghai Aladdin Bio-Chem Technology Co., Ltd (Shanghai, China). *N*-dodecyl mercaptan (98% (mass)) was purchased from Tianjin Chemart Chemical Technology Co., Ltd (Tianjin, China). Deionized water was used in all experiments.

2.2. Preparation of activated sponge

The Jones reagent was prepared based on the previous method [27]. Firstly, 10 g CrO_3 was dissolved in 100 ml deionized water at room temperature, and magnetically stirred for about 30 min to form a transparent orange solution. Then, H_2SO_4 was added into the above solution slowly, then stirred with glass rod. The original PU sponge was etched in Jones reagent for 90 s, then washed sufficiently with deionized water, and dried in vacuum to obtain activated sponge, named Ac-PU.

2.3. Preparation of nanocrystalline Ni-Co LDOs

The total amount of Ni/Co nitrate was controlled to be 10 mmol, and then $Ni(NO_3)_2{\cdot}6H_2O$ and $Co(NO_3)_2{\cdot}6H_2O$ were fully dissolved in 35 ml deionized water under ultrasonic conditions according to the ratios of 2:1 [32]. Then, the 15 mmol of hexamethylenetetramine (HMT) was added into the solution, and the mixture was completely dissolved by ultrasound. After that, the solution was transferred to a Teflon-lined autoclave (100 ml) and reacted for 10 h at 120 °C to obtain Ni-Co LDHs. The Ni-Co LDOs nanocrystals can be obtained by calcining the Ni-Co LDHs at 450 °C.

2.4. Preparation of superhydrophobic PU sponge

A certain amount of Ni-Co LDOs was fully dispersed in acetone with concentration of 3% (mass) under ultrasonic condition. The etched sponge was placed in the above suspension for 5–10 min, then we repeatedly the progress for 5 times to achieve adsorption equilibrium. The loaded sponge with Ni-Co LDOs nanocrystals was obtained by drying. Then, the sponge with Ni-Co LDOs was placed in ethanol solution containing 2.5% (mass) *N*-dodecyl mercaptan for 12 h, and dried in the air to obtain the SS-PU.

2.5. Characterization

The surface morphology of original and superhydrophobic sponges was observed by using the regulus 8100 field emission scanning electron microscope (FE-SEM, Hitachi, Japan). Thermo ESCLAB 250Xi type X-ray photoelectron spectroscopy (XPS) was used to analyze the elemental composition and different chemical environment on the surface of sponges. The FT-IR spectrum information was obtained by Nicolet 6700 infrared spectrometer, which was produced by American Thermo Nicolet Corporation.

SL200KS optical contact angle and interfacial tension meter produced by USA KINO Industry Co., Ltd was used to test the static water contact angle (WCA) and oil contact angle (OCA) of different sponge samples. The volume of single droplet injected by needle

was 5 μl. Each sample was tested at five different positions, and the results were taken as the average value.

2.6. Oil water separation

To separate floating oil on the water surface, the SS-PU was cut into a small piece of 1 cm × 1 cm × 1 cm and contacted with the oil. The oils were dyed by saturated oil red O. For the oil with high density, the SS-PU was immersed to contact with the oil phase underwater. In addition, a large amount of oil–water mixture permeating through the SS-PU was continuously pumped into the collected beaker by peristaltic pump under disturbance and disturbance-free.

3. Results and Discussion

3.1. Design and fabrication of the SS-PU

The preparation of the SS-PU required three steps, the etching of the original sponge, the loading of Ni-Co LDOs and the modification of *n*-dodecyl mercaptan (DDT), as shown in Fig. 1.

To activate the original sponge, the Jones reagent was used to etch the original PU sponge with enough surface area. The etching process could increase surface roughness and generate hydrophilic groups such as —COOH or —OH. When the sponge was under the chromic acid solution, the activation etching changed the composition as well as surface structure, which mainly involved hydrolysis and oxidation process. As shown in Fig. 2(a), the carbamate on the PU sponge hydrolyzed to fracture, producing the corresponding alcohol and carbamate [33]. Meanwhile, under the condition of strong oxidization, the alcohol was oxidized to aldehydes or carboxylic acid at an extraordinarily fast rate. Especially, part of carboxylic acids were further decomposed into CO_2 and other by-products. In addition, due to the instability of the hydrogen on the tertiary carbon, the C—H bond was oxidized to alcohols through intermediates of chromium esters. The alcohols generated products such as olefins, aldehydes, ketones even carboxylic acids [30], as shown in Fig. 2(b). In order to ensure the sufficiency of etched activation and maintain good integrity of three-dimensional framework, the control of etching time was particularly important and accurately designed (Fig. S1, in Supplementary Material).

In this paper, the Ni-Co LDHs were fabricated facilely *via* one-step hydrothermal method, and the reaction mechanism is as shown in Supplementary Material. After the original sponge was etched, its adsorption capacity for transition metal nanoparticles greatly improved. A series of oxidation and hydrolysis reaction occurred in the etching process, which increased the number of polar groups on the surface as well as the roughness of framework, further enhancing the saturation value of sponge in the physical adsorption. As shown in Fig. 3, through a simple dip-coating method, the transition metal oxide nanosheet can be uniformly loaded on the surface of the etched sponge. After being modified by DDT, a long carbon chain would be introduced through RS-M to reduce the surface energy of the sponge. Under the synergistic effect of multi-level roughness and modification of low surface energy, the superhydrophobic surface of sponge would be constructed. Especially, after Ac-PU was immersed in the nanoparticle suspension, it rapidly reached the adsorption equilibrium. In addition, the remaining nanoparticles in the suspension can be recycled. Compared with the *in-situ* growth method of hydrothermal process, this method not only economizes on the cost of synthesis, but provides a valuable application to rapidly prepare superhydrophobic materials in large quantities.

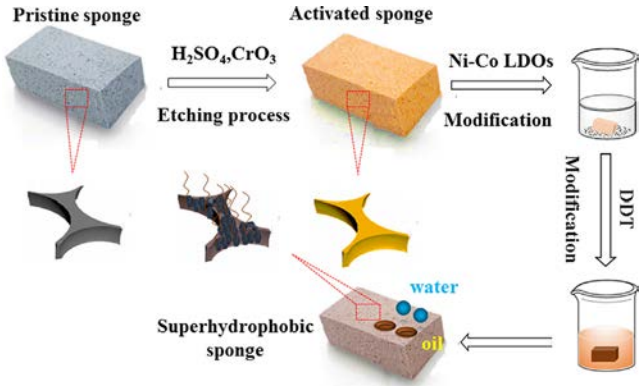

Fig. 1. Schematic illustration of the synthesis process of SS-PU.

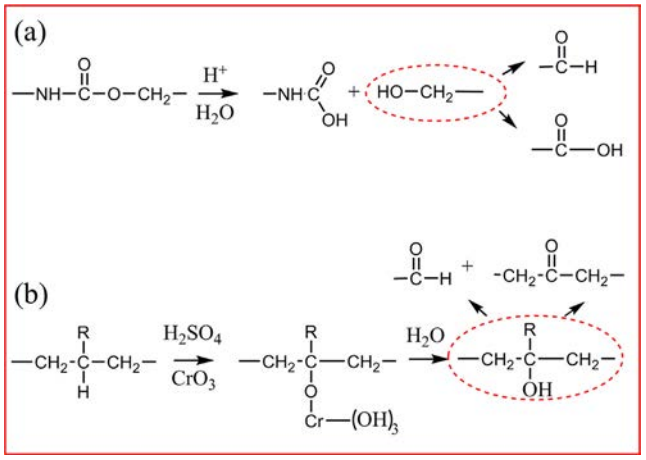

Fig. 2. The main hydrolysis and oxidation reactions of etched process for the pristine PU sponge.

3.2. Characterization

The FT-IR spectra which was used to explore the surface changes of SS-PU sponge are shown in Fig. 4. For the original PU sponge, the band observed at 3284 cm^{-1} corresponds to the stretching vibration of N—H in the polyurethane, while the peaks at 2968 cm^{-1} and 2864 cm^{-1} relate to the stretching vibration, bending vibration of C—H, respectively [34]. The characteristic peaks of 1449 cm^{-1} and 1371 cm^{-1} are the deformation vibration peaks of C—H. The original PU sponge is a kind of polyether type polyurethane which contains plenty of amide structures —NH—C═O and ether bonds C—O—C. The vibration absorption peaks at 1715 cm^{-1} and 1086 cm^{-1} demonstrated the existence of C═O and C—O—C, respectively [35]. After being etched, there were a large number of polar groups on the surface of sponge, including the —COOH. Due to the existence of these groups, a wide and scattered characteristic absorption peak appeared at 3325 cm^{-1} for the activated sponge, corresponding to the stretching vibration of —OH in free or poly carboxylic acid. The peaks of 2920 cm^{-1} and 2850 cm^{-1} relate to the C—H stretching vibration of —CH_3 and —CH_2—, respectively [36]. And the band observed at 1465 cm^{-1} and 721 cm^{-1} corresponds to the deformation vibration absorption peak of —S—CH_2—, the stretching vibration absorption of S—C bond, respectively, indicating that the DDT was successfully grafted on the PU sponge.

XPS measurements confirmed the presence of corresponding group VIII metals, nitrogen, carbon, and oxygen on the etched sponge. The original PU sponge surface only contained three ele-

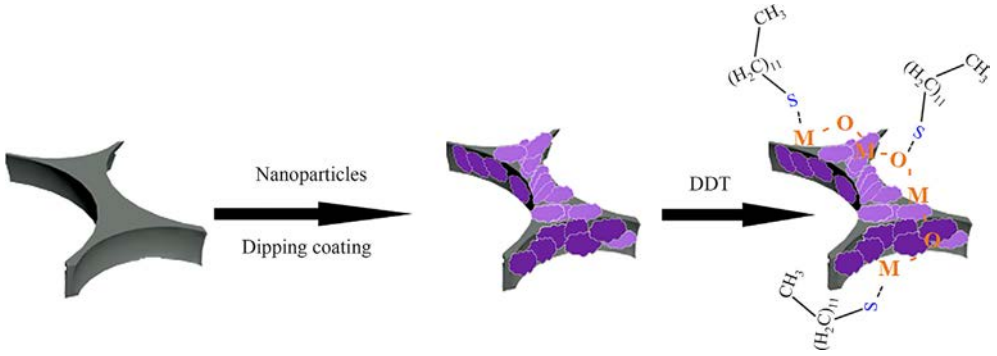

Fig. 3. Schematic illustration of the Ni-Co LDOs coated sponge modified by DDT.

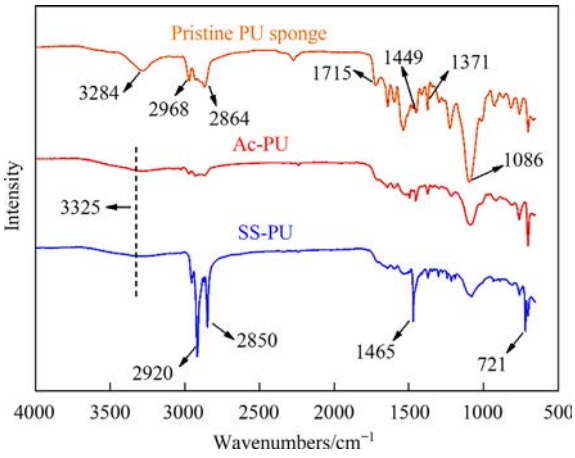

Fig. 4. FT-IR spectra of the pristine PU sponge, Ac-PU and SS-PU.

ments: C, N and O from the full spectrum (Fig. 5(a)), while for the SS-PU sponge, not only elements C and O, but also Ni, Co and S are detected. It is worth noting that the intrinsic N-element signal of sponge skeleton cannot be found due to the Ni-Co LDOs nanoparticles with a certain thickness covering on the surface of activated sponge, which far exceed the detection depth of XPS. Furthermore, the results of C 1s and N 1s of the original sponge with high resolution spectrum were shown in Fig. 5(b)–(c). For C 1s, the absorption peak at 284.6 eV corresponds to C—C and C—H, the absorption peak at 286.4 eV is associated with C—O and C—N, while the absorption peak at 288.8 eV belongs to O=C—O and O=C—N in the form of carbonyl [37]. For N 1s, the fitting of N 1s shows that N only exists in the form of amide. Besides, as shown in Fig. 5(d), Ni 2p is separated into four peaks due to the separation of spin energy at 17.7 eV [38]. The main absorption peaks of Ni $2p_{3/2}$ and Ni $2p_{1/2}$ are 855.9 eV and 873.3 eV, respectively. In addition, the characteristic absorption at 861.4 eV and 879.5 eV comes from the satellite peaks of Ni $2p_{3/2}$ and Ni $2p_{1/2}$, indicating the existence of Ni^{2+} [39]. The fine spectrum of Co 2p is divided into two peaks of different spin orbits and two satellite peaks, as shown in Fig. 5(e). The binding energy of 780.5 eV, 795.6 eV and 782 eV, 797.5 eV correspond to Co^{3+}, Co^{2+}, respectively, which means the existence of Co^{2+} and Co^{3+} in Ni-Co LDOs [40–41]. In addition, only C—C and C—H signal peaks of mercaptan can be probed on the surface of SS-PU (Fig. 5(f)). As shown in Fig. 5(g), the binding energies of $2p_{3/2}$ and $2p_{1/2}$ of S 2p appear at 163.5 eV and 164.8 eV, respectively, while the binding energy of S $2p_{3/2}$ at 163.5 eV is associated with the presence of alkylsulphides, suggesting that the DDT was successfully grafted on the surface of the SS-PU [42]. FT-IR and XPS analysis of the composition of SS-PU both indicated that the successful loading of Ni-Co LDOs precursor and thiol modification. In addition, XRD was used to characterize the crystal structures of LDHs with and LDOs. The prepared Ni Co LDHs showed the characteristic diffraction of Ni-Co hydrotalcite, corresponding to the peak planes of (1 0 1), (0 1 2) and (1 1 0), respectively [43]. When the binary LDHs are calcined, they are transformed into the corresponding binary oxides. The test results are shown in Fig. S2. The red line represents the standard card JCPDS of NiO in cubic phase: 47-1049 [44], and the standard card JCPDS of Co_3O_4 in spinel phase: 73-1702, respectively [45]. And we further explored the morphology of Ni-Co LDOs with different ratio of Ni/Co, as shown in Fig. S3. The conversion of hydroxide to oxide involved recrystallization and the release of gaseous substances, resulting in highly porous texture or hollow structure, but the overall structure did not change [46]. As shown in Fig. S 3(f), when the Ni/Co ratio is 2:1, the prepared precursor has a three-dimensional lamellar structure similar to hydroxide. Therefore, in the preparation process of this experiment, the molar ratio of Ni/Co was set as 2:1.

The surface morphology of the original sponge, activated sponge, Ni-Co LDOs loaded sponge was analyzed by SEM. The pore structure of the original PU sponge was uniform with pore diameter about 400–600 μm (Fig. 6(a)). In addition, the skeleton surface is very smooth, and there are only some folds of polymer film at high magnification as shown in Fig. 6(b). The surface does not have the multi-level rough structure, lacking the condition of modification. However, after etched in Jones reagent, the PU sponge skeleton shrank sharply to form the dense structure (Fig. 6(c)). It can be seen that uneven porous morphology appeared on the surface (Fig. 6(d)). Therefore, the etched rough surface (Ac-PU) facilitates the uniform adsorption of a large number of Ni-Co LDOs precursors. Compared with the activated sponge, the skeleton of loaded sponge is significantly coarse, as shown in Fig. 6(e). However, the low loading capacity of nanoparticles on the surface of the non-etched sponge causes the insufficient uniformity (Fig. 6(g)). As a contrast, the etched sponge skeleton covering with the Ni-Co LDOs presents irregular lamellar structure forming the multistage rough surface (Fig. 6(f)), which provide the indispensable structural condition for superhydrophobic modification. Additionally, the sheets decrease the pore size but do not entirely block the three-dimensional pores, which facilitate the selective permeation of oil phase while repel the water phase. Moreover, CLSM images revealed that the gradually increasing dense coating was on the sponge through two steps of etching and Ni-Co loading, respectively, indicating the enhancement of surface roughness (Fig. S4).

3.3. The wettability

The wettability of sponge surfaces is determined by the cooperation of the chemical composition and the surface roughness [47].

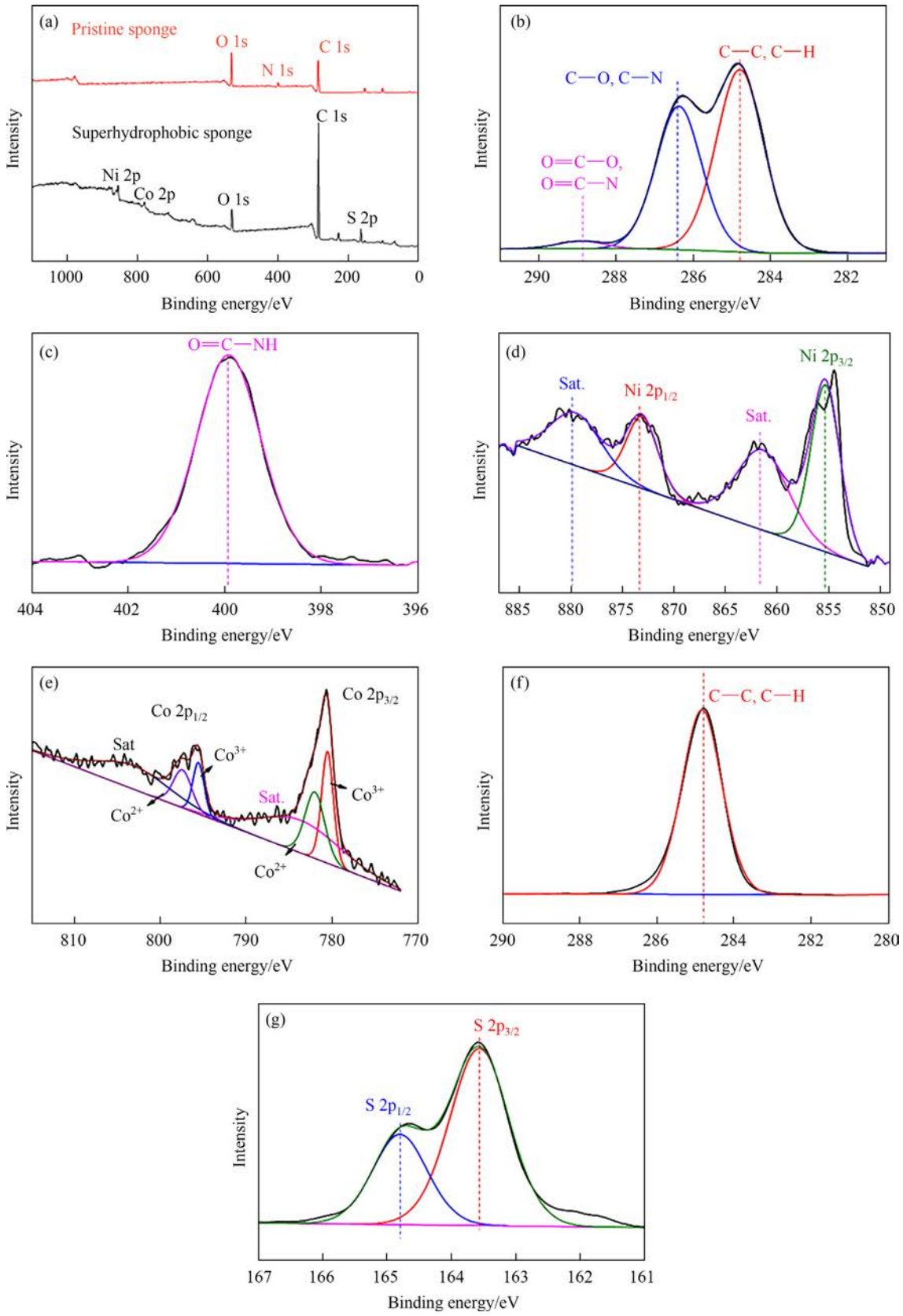

Fig. 5. XPS spectra of the pristine sponge and superhydrophobic sponge. (a) The wide-scan survey spectra, (b)–(c) C 1s and N 1s peak fitting of the pristine sponge, (d)–(g) the Ni 2p, Co 2p, C 1s and S 2p peak fitting of the SS-PU, respectively.

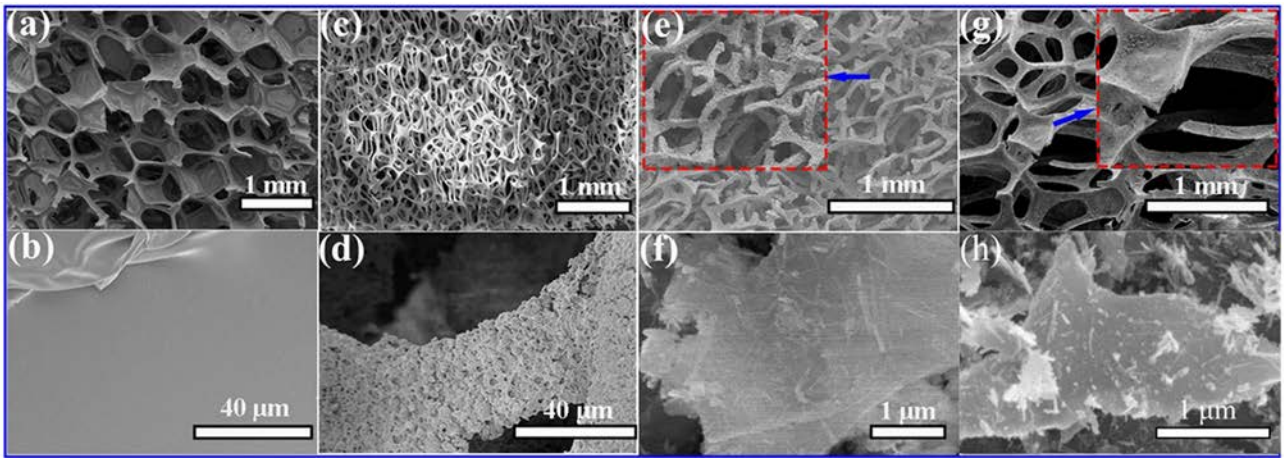

Fig. 6. The SEM images of (a)–(b) the pristine sponge, (c)–(d) the Ac-PU sponge, the Ni-Co LDOs coated sponge (e)–(f) with and (g)–(h) without the etched pretreatment.

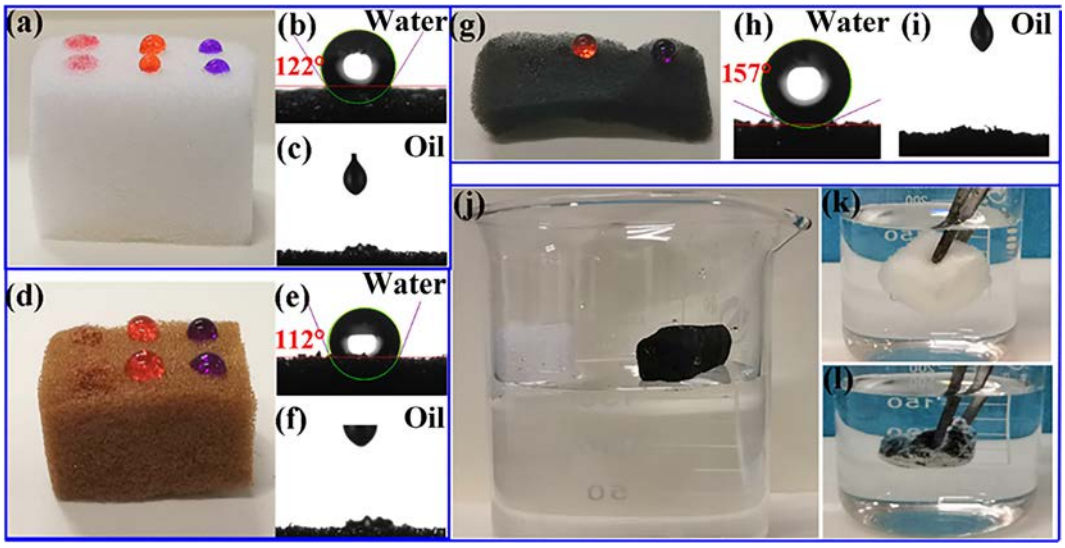

Fig. 7. The WCA and OCA of (a)–(c) the pristine sponge, (d)–(f) the Ac-PU and (g)–(i) SS-PU. (j) The pristine sponge was wetted by the water but the SS-PU floated on the water. (k) The pristine sponge was soaked into the water and (l) the SS-PU immersing into the water with mirror phenomenon.

In order to clearly observe the wettability behavior on the sponge, the water droplets were dyed by methyl orange, bromophenol blue, while the oil droplets were stained by oil red O. Fig. 7(a) illustrates the shape of droplets on the original sponge, of which oil droplets trapped into the sponge completely but all the water droplets kept the state of hemisphere. The original PU sponge of the WCA and OCA are 122° and 0°, respectively, indicating that the hydrophobic and oleophilic property (Fig. 7(b)–(c)). After etched by Jones reagent, the sponge Ac-PU became brown (Fig. 7(d)), and the WCA of etched sponge decreased to 112° while still maintained the super affinity to the oil phase as shown in Fig. 7(e)–(f). In combination with the above characterization analysis, the increasement of roughness, generation of a large number of polar groups on the surface of PU sponge both results in the further enhancement of hydrophilicity of the activated sponge. When loaded by Ni-Co LDOs and modified by DDT, the wettability of the sponge altered inversely. The spherical oil droplets with WCA of 157° on the sponge (Fig. 7(h)) indicates that SS-PU has superhydrophobic property, while the OCA of 0° in the air show the oleophilicity (Fig. 7(i)). After the sponges were placed in water for a long time, the bottom of original sponge was slowly wetted, but the SS-PU floated stably on the water surface without occurring any wetting behavior, as shown in Fig. 7(g)–(l). In addition, it is obvious that there is a silver mirror-like film covering on the surface, which can be explained as the extremely strong repulsive force of a large amount of air captured by the rough nano structure of the SS-PU to the water phase.

Then, we used SL200KS with high-speed photography system to investigate the dynamic wetting behavior of the SS-PU with a certain tilted angle (about 25°). For the original sponge, as shown in Fig. 8(a), when the water droplet is injected to drop onto the sponge, it is firmly bound on the surface with a hemispherical state, leaving no sign of rolling, which demonstrate the strong adhesion of the original sponge towards the water. However, for the SS-PU, the water droplet rolled off easily on the tilted surface by gravity without adhesion. It only took 29.7 ms from the top to the bottom edge, as shown in Fig. 8(b), which also verified the ultra-low adhesion characteristics of the as-prepared superhydrophobic surface to the water phase.

3.4. The self-cleaning effect and oil absorption performance

Due to the low WCA hysteresis of superhydrophobic materials, water droplets roll off the surface rapidly to remove the pollutants

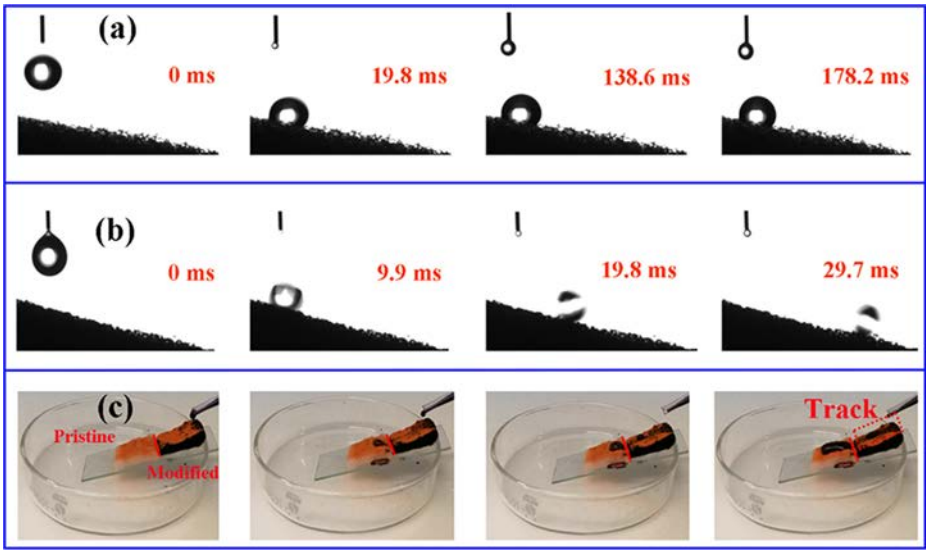

Fig. 8. Water droplet rolled down along the sloping surface of (a) the pristine sponge and (b) the SS-PU. (c) The test of the self-cleaning effect for superhydrophobic and pristine surface.

on the surface for achieving self-cleaning [48]. Compared with the original sponge, the as-prepared SS-PU has the self-cleaning effect similar to the lotus leaf surface, as shown in Fig. 8(c). The superhydrophobic sponge and original sponge were both placed on a transparent glass slide with a small tilted angle. The flowing water droplets can easily take away the contaminants (methyl orange powder) on the surface of SS-PU, leaving a clear rolling track (black). However, as a contrast, the mixtures of water droplets and powders flowing from the side of SS-PU are adhered to the surface of the original sponge. Based on the above phenomenon, it can be seen that the SS-PU has strong repulsion and low adhesion to the water phase, performing its good self-cleaning ability which is crucial to remove contaminants residing on the sponge surface.

In order to study the adsorption capacity, we chose six types of oils (*n*-hexane, kerosene, diesel oil, petroleum ether, dichloromethane, soybean oil) as model absorbates. The SS-PU was dropped to contact with the above oils for some time to ensure the absorption saturation. The parameter A_m defined as the mass ratio of the adsorbed oil phase to the initiative SS-PU is employed to investigate the oil absorption capacity, as shown in Eq. (1):

$$A_m = (M_1 - M_0)/M_0$$

Here, the M_1 stands for the mass of the SS-PU after saturated absorption, and the M_0 is the mass of original SS-PU. In fact, different types of oils with diverse viscosity and density led to various adsorption performance. Fig. 9 shows the adsorption value A_m of the SS-PU for different model absorbates, and the absorption capacity varied from 26 to 44.8. The higher viscosity has the greater absorption capacity A_m, while the oil droplets with the lower viscosity trapped in the sponge channel flowed more easily which caused the loss of adsorption capacity. In particular, the SS-PU adsorbed the large amount of soybean oil, which was about the 44.8 times mass of the sponge, indicating the promising prospect for the treatment of oil spill. For *n*-hexane and petroleum ether, the relatively low absorption may result from both their low density and rapid evaporation" [5].

3.5. Oil/water separation

Generally, separation performance of porous materials with superhydrophobicity is assessed by separating oil/water mixtures [49]. The light oil (*n*-hexane) and the heavy oil (dichloromethane)

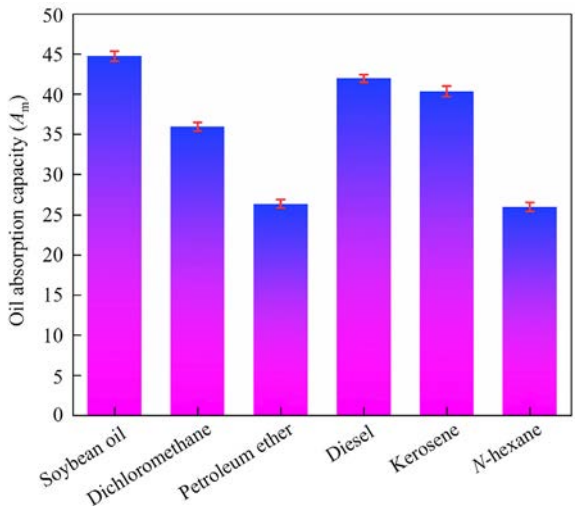

Fig. 9. The oil absorption capacity of the as-prepared SS-PU for various sample oils.

both were chosen as model oils. As shown in Fig. 10(a), when the SS-PU touched the surface of the floating *n*-hexane, the rapid absorption occurred due to the combination of its high porosity, hierarchical structure and superoleophilic nature [50]. In addition, *n*-hexane layer on the surface of sponge further permeated to the interior skeleton by the capillary force, which promoted the continuous oil absorption. By using tweezers to move the sponge in the vessel, oils were completely absorbed in a few seconds, resulting in a transparent region of clean water. In fact, *n*-hexane can be conveniently recycled by squeezing the sponge, and the extruded SS-PU after several adsorption cycles can also be reused *via* simple drying.

The SS-PU is also employed to absorb the heavy oil. When the clean SS-PU was immersed into the water, the mirror-like surface showed the good superhydrophobic performance. Once wetted by the oil droplet, the trapped air bubbles in the space of the sponge framework were replaced by the adsorbed dichloromethane, while the silver mirror disappeared (Fig. 10(b)). The oil droplets that removed by adsorption can be extruded for recycling as well. The adsorption and recycling of light and heavy oils exhib-

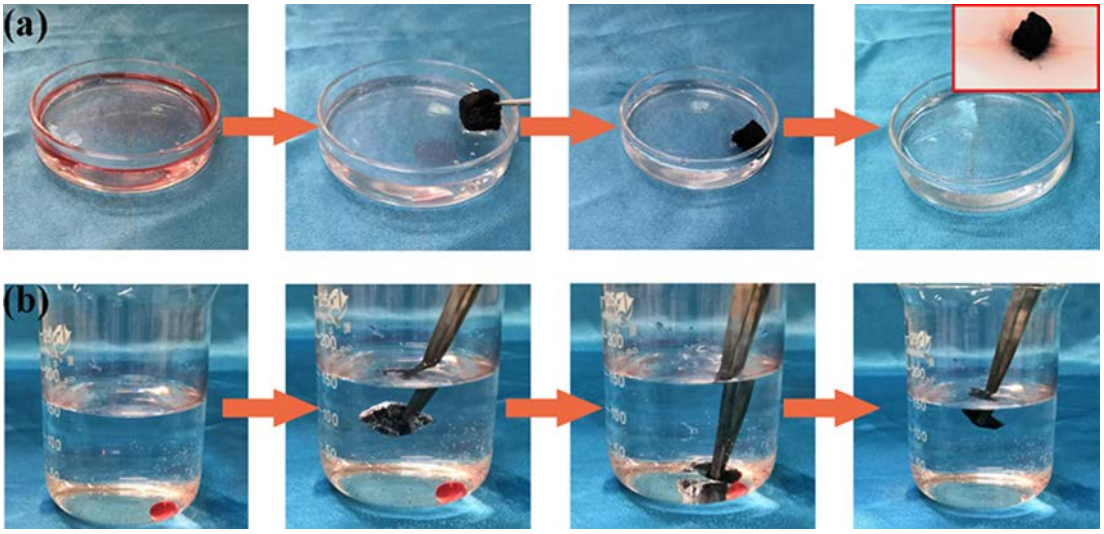

Fig. 10. (a) Dynamic absorption process of oil removal of *n*-hexane (dyed with oil red) from the water surface and (b) dichloromethane (dyed with oil red) from the bottom of water by SS-PU.

ited the highly efficient ability in oil/water separation, which is expected to show great application value in the treatment of marine crude oil pollution and domestic oily wastewater.

The designed device as shown in Fig. S5 was further used to achieve continuous oil/water separation. The SS-PU was tightly filled into the inlet hose of the peristaltic pump, fixed with tape and iron clip, which was extended to the oil/water interface, and the outlet was connected to the empty beaker for oil phase collection. When the peristaltic pump was started, the *n*-hexane (dyed in red) in the oil/water mixture was continuously transformed into the beaker, while the water phase was repelled by the SS-PU because of the superhydrophobic surface. All the *n*-hexane floating on the water was absorbed by the sponge and transported to the beaker, but no water phase could be found in the collected *n*-hexane, showing the high absorption capacity and efficient separation.

In the practical environment, the separation process is often affected by severe disturbance. Therefore, we designed a device system to achieve continuous separation under the condition of turbulent vortex *via* using magnetic stirrer and peristaltic pump (Fig. 11). However, the turbulence did not influence the absorption performance, while the SS-PU still maintained the efficient separation and great robustness. The excellent stability indicates that the SS-PU successfully adapt to the continuous oil–water separation under disturbed conditions, showing its potential value of industrial application.

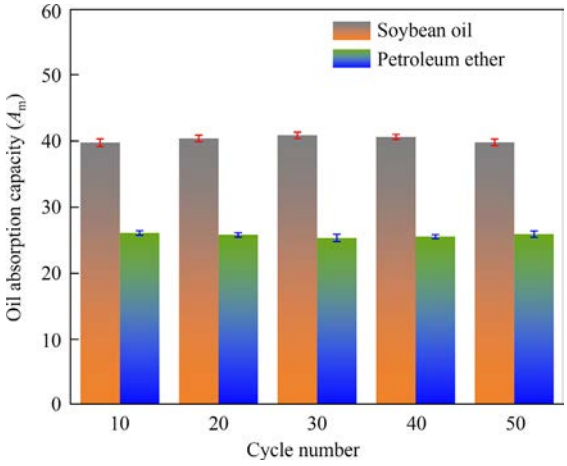

Fig. 12. Oil absorption capacity (soybean oil and petroleum ether) for different recycle use.

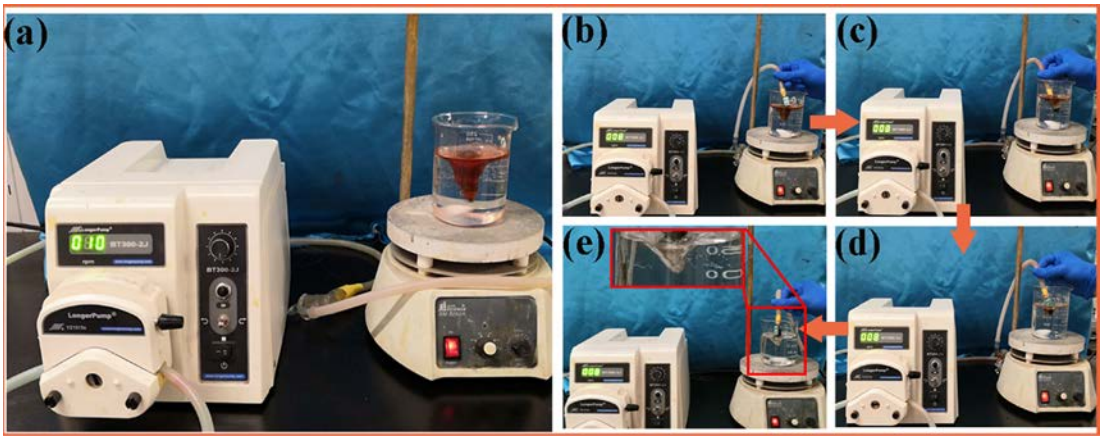

Fig. 11. The designed device system and continuous oil removal process under the condition of disturbance.

3.6. Reusability and durability

The strong durability and reusability for the superhydrophobic materials is significantly necessary [51]. In order to evaluate the reusability performance of the as-prepared SS-PU, the A_m value of the sponge was recorded. After each oil absorption test, the SS-PU was fully squeezed and the residual oil adsorbed in the sponge was collected until no excess oil spillage. The soybean oil and petroleum ether were selected as the test oil, and the oil absorption capacity A_m of SS-PU within 50 cycles is as shown in Fig. 12. Notably, there was no significant difference among various cycles (Fig. 9). However, after 50 times of absorption-squeezing recycling, the SS-PU still had stable oil absorption capacity, showing excellent reusability performance.

Here, we utilized the micro morphology and static CA of the surface of SS-PU after different oil absorption tests (petroleum ether) to investigate the robustness and durability (Fig. S6). The SEM images show that there was no obvious change in morphology of Ni-Co LDOs nanocrystals on the sponge skeleton after different cycles. A large number of micro sheets and spheres with different sizes still densely covered the sponge skeleton after 50 cycles. The particles that adhered to the surface of SS-PU partly fell off during absorption-squeezing recycling, but multi-level structures anchored on the activated sponge were not destroyed. The stability of the structure benefits from the polar surface created by etching step which greatly enhanced the adsorption of transition metal oxide nanoparticles. The stable micro-nano hierarchical structure and covalent grafted molecules of DDT further endowed the SS-PU with good stability and durability of absorption. After 100 times cycles of oil absorption, the CA of SS-PU decreased from 157° to 152° but still maintained strong hydrophobic characteristic in long-term operation. Nevertheless, when the number of cycles gradually increased to 150, the contact angle of water eventually decreased to 145°. Based on the above experiment, the SS-PU displays good reusability and durability, which can broaden the application to fabricate the hydrophobic materials in oil/water separation. In order to test its stability in acid and alkali solution, we immersed the sample into aqueous solution of pH of 1 and 14 for 24 h, respectively. And we examined its contact angles, the corresponding results without obvious decline are shown in Fig. S7. Because of good stability for Ni-Co LDOs, the as-prepared superhydrophobic foam can resist acid and alkali environment.

4. Conclusions

In this paper, we demonstrate a facile approach to synthesizing the SS-PU sponge through the activation etching, the loading of Ni-CO LDOs nanocrystals and the modification of DDT. The morphology and hydrophobic property were controlled by activation time to achieve ideal superhydrophobicity. The constructed sponge endows with excellent selectivity and good oil absorption capacities, which can be widely used in absorbing various types of oils. In addition, it not only effectively treats floating oil on the water surface, but also quickly absorbs heavy oil underwater. Besides, the ultra-low adhesion of the SS-PU to water exhibits excellent self-cleaning performance, which is capable of clearing the pollutants. Especially, in our designed system, the SS-PU sponge exhibits effective and stable oil absorption against the condition of turbulent disturbance due to the excellent stability. The as-prepared sponge still has strong oil absorption ability in 150 cycles, maintaining the complete hierarchical structure, which show outstanding durability in long-term operation and indicate an applied prospect in practical industry.

Data availability

No data was used for the research described in the article.

Declaration of Competing Interest

The authors declare that they have no known competing financial interests or personal relationships that could have appeared to influence the work reported in this paper.

Acknowledgements

We are grateful for the financial support from National Key Research & Development Program of China (2017B0602702)

Supplementary Material

Supplementary data to this article can be found online at https://doi.org/10.1016/j.cjche.2022.03.023.

References

[1] Y.Y. Chen, A.T. Xie, J.Y. Cui, J.H. Lang, Y.S. Yan, C.X. Li, J.D. Dai, UV-driven antifouling paper fiber membranes for efficient oil-water separation, *Ind. Eng. Chem. Res.* 58 (13) (2019) 5186–5194.
[2] X. Deng, J.S. Zhang, L.R. Zhang, G.R. Cheng, B.H. Chen, Y.Y. Zhang, G.H. Gao, Poly (ionic liquid)-coated meshes with opposite wettability for continuous oil/water separation, *Ind. Eng. Chem. Res.* 59 (14) (2020) 6672–6680.
[3] M.D. Sosa, A. Canneva, A. Kaplan, N.B. D'Accorso, R.M. Negri, From superhydrophilic to superhydrophobic polymer-nanoparticles coated meshes for water-oil separation systems with resistance to hard water, *J. Petroleum Sci. Eng.* 194 (2020).
[4] Y.J. Xiong, B.Q. Wu, X.F. Huang, C.L. Li, B. Lu, J. Liu, L.J. Lu, S.Y. Li, K.M. Peng, Coupling magnetic particles with flocculants to enhance demulsification and separation of waste cutting emulsion for engineering applications, *J. Environ. Sci. (China)* 105 (2021) 173–183.
[5] C. Ong, Y. Shi, J. Chang, F. Alduraiei, N. Wehbe, Z. Ahmed, P. Wang, Tannin-inspired robust fabrication of superwettability membranes for highly efficient separation of oil-in-water emulsions and immiscible oil/water mixtures, *Sep. Purif. Technol.* 227 (2019) 115657.
[6] Y.Y. Chen, A.T. Xie, J.Y. Cui, J.H. Lang, C.X. Li, Y.S. Yan, J.D. Dai, One-step facile fabrication of visible light driven antifouling carbon cloth fibers membrane for efficient oil-water separation, *Sep. Purif. Technol.* 228 (2019).
[7] C.C. Ma, Y.J. Li, P. Nian, H.O. Liu, J.S. Qiu, X.F. Zhang, Fabrication of oriented metal-organic framework nanosheet membrane coated stainless steel meshes for highly efficient oil/water separation, *Sep. Purif. Technol.* 229 (2019).
[8] M.O. Adebajo, R.L. Frost, J.T. Kloprogge, O. Carmody, S. Kokot, Porous materials for oil spill cleanup: A review of synthesis and absorbing properties, *J. Porous Mater.* 10 (2003) 159–170.
[9] N. Pino, T. Bui, G. Hincapié, D. López, D.E. Resasco, Hydrophobic zeolites for the upgrading of biomass-derived short oxygenated compounds in water/oil emulsions, *Appl. Catal. A Gen.* 559 (2018) 94–101.
[10] Z.Y. Xu, H. Zhou, S.C. Tan, X.D. Jiang, W.B. Wu, J.T. Shi, P. Chen, Ultralight superhydrophobic carbon aerogels based on cellulose nanofibers/poly(vinyl alcohol)/graphene oxide (CNFs/PVA/GO) for highly effective oil-water separation, *Beilstein J. Nanotechnol.* 9 (2018) 508–519.
[11] D. Hady, R.F. Susanti, A.A. Arie, Preparation of activated carbons originated from orange peel waste by subcritical H_2O activation method, *IOP Conf. Ser. Mater. Sci. Eng.* 742 (1) (2020).
[12] Y.X. Jin, P. Jiang, Q.P. Ke, F.H. Cheng, Y. Zhu, Y.X. Zhang, Superhydrophobic and superoleophilic polydimethylsiloxane-coated cotton for oil-water separation process: An evidence of the relationship between its loading capacity and oil absorption ability, *J. Hazard. Mater.* 300 (2015) 175–181.
[13] H. Liu, Y. Kang, Superhydrophobic and superoleophilic modified EPDM foam rubber fabricated by a facile approach for oil/water separation, *Appl. Surf. Sci.* 451 (2018) 223–231.
[14] X. Long, Z.L. Wang, S. Xiao, Y.M. An, S.H. Yang, Transition metal based layered double hydroxides tailored for energy conversion and storage, *Mater. Today* 19 (4) (2016) 213–226.
[15] G.L. Fan, F. Li, D.G. Evans, X. Duan, Catalytic applications of layered double hydroxides: Recent advances and perspectives, *Chem. Soc. Rev.* 43 (20) (2014) 7040–7066.
[16] L. Zhu, H. Li, Y.Y. Yin, Z.Z. Cui, C. Ma, X.F. Li, Q.Z. Xue, One-step synthesis of a robust and anti-oil-fouling biomimetic cactus-like hierarchical architecture for highly efficient oil/water separation, *Environ. Sci.: Nano* 7 (3) (2020) 903–911.
[17] M. Daud, A. Hai, F. Banat, M.B. Wazir, M. Habib, G. Bharath, M.A. Al-Harthi, A review on the recent advances, challenges and future aspect of layered double hydroxides (LDH) - Containing hybrids as promising adsorbents for dyes removal, *J. Mol. Liq.* 288 (2019).

[18] G. Mishra, B. Dash, S. Pandey, Layered double hydroxides: A brief review from fundamentals to application as evolving biomaterials, *Appl. Clay Sci.* 153 (2018) 172–186.
[19] G. Nagaraju, G.S.R. Raju, Y.H. Ko, J.S. Yu, Hierarchical Ni–Co layered double hydroxide nanosheets entrapped on conductive textile fibers: A cost-effective and flexible electrode for high-performance pseudocapacitors, *Nanoscale* 8 (2) (2016) 812–825.
[20] X.J. Liu, L. Ge, W. Li, X.Z. Wang, F. Li, Layered double hydroxide functionalized textile for effective oil/water separation and selective oil adsorption, *ACS Appl. Mater. Interfaces* 7 (1) (2015) 791–800.
[21] G.M. Jiang, W.Y. Fu, S. Shu, Z.Y. Zhang, S. Zhang, Y.X. Zhang, X.M. Zhang, F. Dong, X.S. Lv, MgAl layered double oxide: One powerful sweeper of emulsified water and acid for oil purification, *J. Hazard. Mater.* 367 (2019) 658–667.
[22] X.T. Hou, S.Q. Liu, C.Z. Yu, L.K. Jiang, Y.J. Zhang, G.C. Liu, C.Z. Zhou, T. Zhu, Y.J. Xin, Q.H. Yan, A novel magnetic CuFeAl-LDO catalyst for efficient degradation of tetrabromobisphenol a in water, *Chem. Eng. J.* 430 (2022) 133107.
[23] M. Peng, Y. Zhu, H. Li, K. He, G.M. Zeng, A.W. Chen, Z.Z. Huang, T.T. Huang, L. Yuan, G.Q. Chen, Synthesis and application of modified commercial sponges for oil-water separation, *Chem. Eng. J.* 373 (2019) 213–226.
[24] L.H. Zhang, L.D. Xu, Y.L. Sun, N. Yang, Robust and durable superhydrophobic polyurethane sponge for oil/water separation, *Ind. Eng. Chem. Res.* 55 (43) (2016) 11260–11268.
[25] Y. Zhou, N. Zhang, X. Zhou, Y.B. Hu, G.Z. Hao, X.D. Li, W. Jiang, Design of recyclable superhydrophobic PU@Fe_3O_4@PS sponge for removing oily contaminants from water, *Ind. Eng. Chem. Res.* 58 (8) (2019) 3249–3257, https://doi.org/10.1021/acs.iecr.8b04642.
[26] Q. Zhu, Q.M. Pan, F.T. Liu, Facile removal and collection of oils from water surfaces through superhydrophobic and superoleophilic sponges, *J. Phys. Chem. C* 115 (35) (2011) 17464–17470.
[27] J. Li, L. Shi, Y. Chen, Y.B. Zhang, Z.G. Guo, B.L. Su, W.M. Liu, Stable superhydrophobic coatings from thiol-ligand nanocrystals and their application in oil/water separation, *J. Mater. Chem.* 22 (19) (2012) 9774.
[28] Q. Zhu, Y. Chu, Z.K. Wang, N. Chen, L. Lin, F.T. Liu, Q.M. Pan, Robust superhydrophobic polyurethane sponge as a highly reusable oil-absorption material, *J. Mater. Chem. A* 1 (17) (2013) 5386.
[29] L. Wu, L.X. Li, B.C. Li, J.P. Zhang, A.Q. Wang, Magnetic, durable, and superhydrophobic polyurethane@Fe_3O_4@SiO_2@fluoropolymer sponges for selective oil absorption and oil/water separation, *ACS Appl. Mater. Interfaces* 7 (8) (2015) 4936–4946.
[30] X.Y. Zhang, Z. Li, K.S. Liu, L. Jiang, Bioinspired multifunctional foam with self-cleaning and oil/water separation, *Adv. Funct. Mater.* 23 (22) (2013) 2881–2886.
[31] B. Wang, J. Li, G.Y. Wang, W.X. Liang, Y.B. Zhang, L. Shi, Z.G. Guo, W.M. Liu, Methodology for robust superhydrophobic fabrics and sponges from *in situ* growth of transition metal/metal oxide nanocrystals with thiol modification and their applications in oil/water separation, *ACS Appl. Mater. Interfaces* 5 (5) (2013) 1827–1839.
[32] J. Zhang, F. Liu, J.P. Cheng, X.B. Zhang, Binary nickel-cobalt oxides electrode materials for high-performance supercapacitors: Influence of its composition and porous nature, *ACS Appl. Mater. Interfaces* 7 (32) (2015) 17630–17640.
[33] R.A. Evangelista, M.V. Sefton, Coating of two polyetoer-polyurethanes and polyethylene with a heparin-poly-(vinyl alcohol) hydrogel, *Biomaterials 7(3)* (1986) 206–211.
[34] E. Yilgör, E. Burgaz, E. Yurtsever, İ. Yilgör, Comparison of hydrogen bonding in polydimethylsiloxane and polyether based urethane and urea copolymers, *Polymer* 41 (3) (2000) 849–857.
[35] J.P. Santerre, R.S. Labow, The effect of hard segment size on the hydrolytic stability of polyether-urea-urethanes when exposed to cholesterol esterase, *J. Biomed. Mater. Res.* 36 (2) (1997) 223–232.
[36] M.F. Calderón, E. Zelaya, G.A. Benitez, P.L. Schilardi, A.H. Creus, A.G. Orive, R.C. Salvarezza, F.J. Ibañez, New findings for the composition and structure of Ni nanoparticles protected with organomercaptan molecules, *Langmuir* 29 (15) (2013) 4670–4678.
[37] C. Yu, Z.B. Liu, X.T. Han, H.W. Huang, C.T. Zhao, J. Yang, J.S. Qiu, NiCo-layered double hydroxides vertically assembled on carbon fiber papers as binder-free high-active electrocatalysts for water oxidation, *Carbon* 110 (2016) 1–7.
[38] X. Ye, Z.M. Jiang, L.X. Li, Z.H. Xie, *In-situ* growth of NiAl-layered double hydroxide on AZ31 Mg alloy towards enhanced corrosion protection, *Nanomaterials (Basel)* 8 (6) (2018) 411.
[39] L. Li, K.S. Hui, K.N. Hui, Y.R. Cho, Ultrathin petal-like NiAl layered double oxide/sulfide composites as an advanced electrode for high-performance asymmetric supercapacitors, *J. Mater. Chem. A* 5 (37) (2017) 19687–19696.
[40] R.C. Li, Z.X. Hu, X.F. Shao, P.P. Cheng, S.S. Li, W.D. Yu, W.R. Lin, D.S. Yuan, Large scale synthesis of NiCo layered double hydroxides for superior asymmetric electrochemical capacitor, *Sci. Rep.* 6 (2016) 18737.
[41] J.W. Nai, H.J. Yin, T.T. You, L.R. Zheng, J. Zhang, P.X. Wang, Z. Jin, Y. Tian, J.Z. Liu, Z.Y. Tang, L. Guo, Efficient electrocatalytic water oxidation by using amorphous Ni-Co double hydroxides nanocages, *Adv. Energy Mater.* 5 (10) (2015) 1401880.
[42] Y.L. Shi, W. Yang, X.J. Feng, Y.S. Wang, G.R. Yue, S.P. Jin, Fabrication of superhydrophobic-superoleophilic copper mesh *via* thermal oxidation and its application in oil-water separation, *Appl. Surf. Sci.* 367 (2016) 493–499.
[43] L.Y. Jiang, Y.W. Sui, J.Q. Qi, Y. Chang, Y.Z. He, Q.K. Meng, F.X. Wei, Z. Sun, Y.X. Jin, Hierarchical Ni-Co layered double hydroxide nanosheets on functionalized 3D-RGO films for high energy density asymmetric supercapacitor, *Appl. Surf. Sci.* 426 (2017) 148–159.
[44] R. Zhang, J.W. Shi, T.T. Zhou, J.C. Tu, T. Zhang, A yolk-double-shelled heterostructure-based sensor for acetone detecting application, *J. Colloid Interface Sci.* 539 (2019) 490–496.
[45] L.T. Yang, B.G. Zhang, B. Fang, L.G. Feng, A comparative study of $NiCo_2O_4$ catalyst supported on Ni foam and from solution residuals fabricated by a hydrothermal approach for electrochemical oxygen evolution reaction, *Chem. Commun. (Camb)* 54 (93) (2018) 13151–13154.
[46] J.P. Cheng, Q.L. Shou, J.S. Wu, F. Liu, V.P. Dravid, X.B. Zhang, Influence of component content on the capacitance of magnetite/reduced graphene oxide composite, *J. Electroanal. Chem.* 698 (2013) 1–8.
[47] C.L. Chen, D. Weng, A. Mahmood, S. Chen, J.D. Wang, Separation mechanism and construction of surfaces with special wettability for oil/water separation, *ACS Appl. Mater. Interfaces* 11 (11) (2019) 11006–11027.
[48] C. Jiang, W.Q. Liu, M.P. Yang, C.H. Liu, S. He, Y.K. Xie, Z.F. Wang, Robust multifunctional superhydrophobic fabric with UV induced reversible wettability, photocatalytic self-cleaning property, and oil-water separation *via* thiol-ene click chemistry, *Appl. Surf. Sci.* 463 (2019) 34–44.
[49] Q.P. Ke, Y.X. Jin, P. Jiang, J. Yu, Oil/water separation performances of superhydrophobic and superoleophilic sponges, *Langmuir* 30 (44) (2014) 13137–13142.
[50] X. Zhang, B. Wang, X.M. Qin, S.H. Ye, Y.T. Shi, Y.Z. Feng, W.J. Han, C.T. Liu, C.Y. Shen, Cellulose acetate monolith with hierarchical micro/nano-porous structure showing superior hydrophobicity for oil/water separation, *Carbohydr. Polym.* 241 (2020).
[51] Y. Xie, Y.H. Gu, J. Meng, X. Yan, Y. Chen, X.J. Guo, W.Z. Lang, Ultrafast separation of oil/water mixtures with layered double hydroxide coated stainless steel meshes (LDH-SSMs), *J. Hazard. Mater.* 398 (2020) 122862.